Clinical Biomechanics 61 (2019) 31–37

Contents lists available at ScienceDirect

Clinical Biomechanics

journal homepage: www.elsevier.com/locate/clinbiomech

‘Pre-launch’ finite element analysis of a short-stem total hip arthroplasty system consisting of two implant types

Matthias Lerch[a,*], Henning Windhagen[a], Agnes-Elisabeth Kurtz[a], Stefan Budde[a], Bernd-Arno Behrens[b], Anas Bouguecha[b,c], Amer Almohallami[b,d]

[a] Department of Orthopaedic Surgery, Hannover Medical School, Anna-von-Borries Straße 1-7, 30625 Hannover, Germany
[b] Institute of Forming Technology and Machines, Leibniz University Hannover, An der Universität 2, 30823 Garbsen, Germany
[c] Laboratory La2MP, ENIS, National school of engineering in Gafsa, Sfax, Tunisia
[d] PROFIL Verbindungstechnik GmbH & Co. KG, Otto-Hahn-Strasse 22-24, 61381 Friedrichsdorf, Germany

ARTICLE INFO

Keywords:
Total hip arthroplasty
Short-stemmed implant
Finite element analysis
Bone remodeling

ABSTRACT

Background: We applied a previously established and validated numerical model to a novel short-stemmed implant for a ‘pre-launch’ investigation.
Methods: The implant system consists of two different implant geometries for valgus/varus-positioned proximal femurs with differences in volume distribution, head/neck angle, and calcar alignment. The aim of the design was to achieve a better adaption to the anatomic conditions, resulting in a favourable load transfer. The implant type G showed the best fit to our model, but both stem geometries were implanted; the implant type B was used to compute an ‘imperfection scenario’.
Findings: Apparent bone density decreased by 4.3% in the entire femur with the implant type G, and by 12.3% with the implant type B. Bone mass loss was pronounced in the proximal calcar region. Apparent bone density increased at the lateral cortical ring and in the minor trochanter. The apparent bone density in the imperfection scenario was very similar to that of a straight stem, indicating a distal load transfer.
Interpretation: No adverse effects of the A2 short-stemmed implant system on bone remodeling could be detected. The overall bone density reduction was acceptable, and wedge fixation was not observed, indicating that there was no distal load transfer. The simulation of an incongruous implant indicates the sensitivity of our model in response to modifications of implant positioning. Correct implant selection and positioning is crucial when using the A2 system.

1. Introduction

The indications for Total Hip Arthroplasty (THA) are continuously expanding. > 20% of patients receiving joint arthroplasty are younger than 60 years (Jerosch, 2011). So called “neck preserving” short stems where developed for these patients as they are meant to avoid stress shielding and increase periprosthetic bone formation in the proximal femur to facilitate necessary revision procedures (Lerch et al., 2012a). One of the most important reasons for femoral bone loss is non-physiologic load transfer and associated stress shielding (Goetzen et al., 2005). It occurs in the periprosthetic bone and depends on stress distribution due to implant design. We know that a longer implant might cause distal load transfer, causing stress shielding and consecutive bone loss in the proximal femur (Lerch et al., 2012b; Sano et al., 2008; Stukenborg-Colsman et al., 2012; Tai et al., 2003). In an analysis of a stemless femoral implant, stress shielding was significantly reduced as compared to that of a conventional straight stem (Tai et al., 2003). FE analysis of the Thrust Plate Prosthesis (Centerpulse Orthopedics, Winterthur, Switzerland), which was developed to transmit load more physiologically, showed increased bone formation in the medial proximal region of the femur (Lerch et al., 2012a; Taylor et al., 2004).

In the present study, we performed a finite element analysis of a novel short-stemmed total hip arthroplasty (THA) implant before market launch. The prosthesis is optimized concerning offset, leg length reconstruction, and calcar alignment. The ‘two body’ design philosophy consists of two different implants with two different geometries for valgus/varus-positioned proximal femurs, with differences in volume distribution, head/neck angle, and calcar alignment. This is achieved by

* Corresponding author.
E-mail addresses: Matthias.lerch@diakovere.de (M. Lerch), henning.windhagen@diakovere.de (H. Windhagen), agneselisabeth.kurtz@diakovere.de (A.-E. Kurtz), stefan.budde@diakovere.de (S. Budde), behrens@ifum.uni-hannover.de (B.-A. Behrens).

https://doi.org/10.1016/j.clinbiomech.2018.11.002
Received 18 February 2018; Accepted 6 November 2018

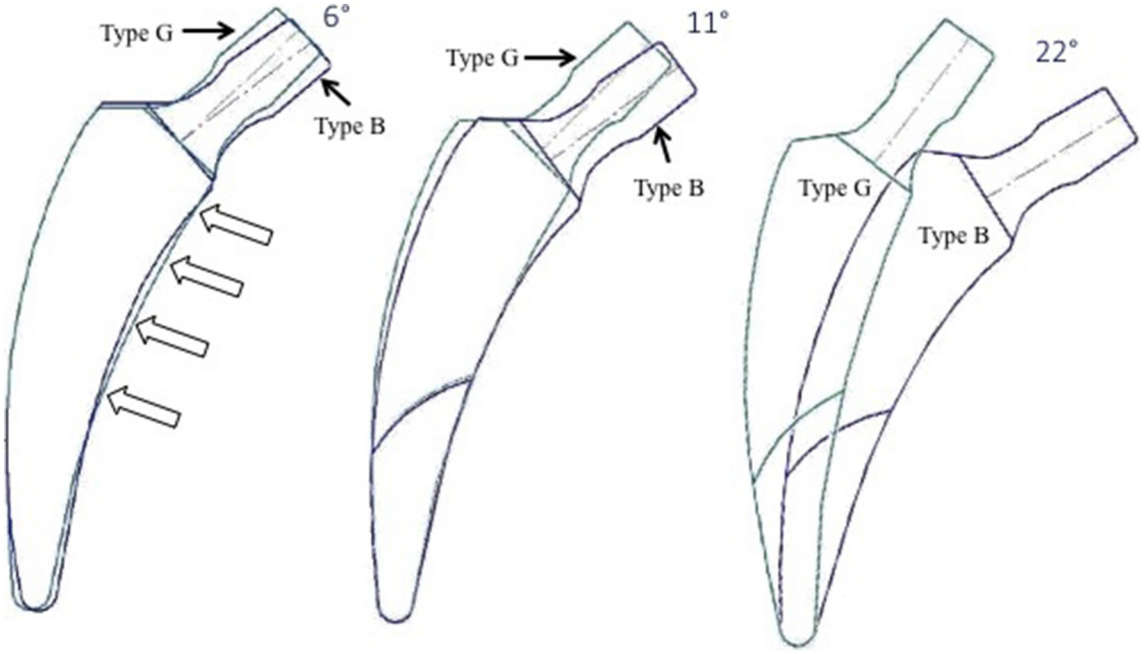

Fig. 1. Comparison of the base implant types G and B of the A2 total hip arthroplasty short-stem system. The bold arrows mark the difference in calcar alignment (a). The difference in the neck angle is 6°. In (b) the lateral distal smooth parts of both stems are aligned to point up the difference in varus/valgus positioning of 11°. A difference of up to 22° is possible when the tips are aligned (c).

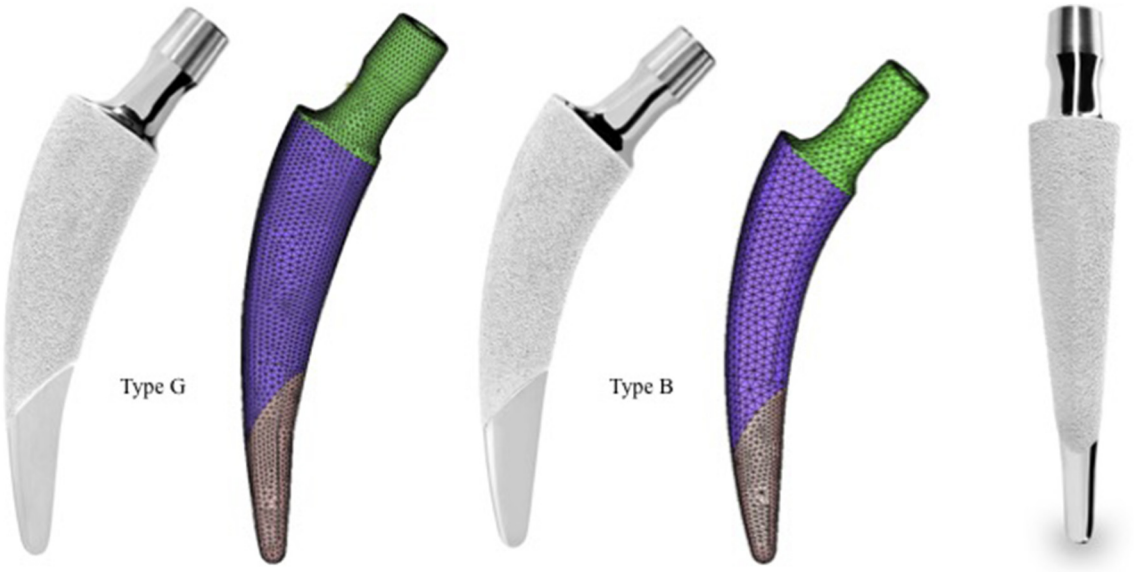

Fig. 2. Anteroposterior view of the base of implant types G and B (original on the left, finite element model on the right). The axial profile of both implant types is identical (b).

size evolution that implements a gradual increase in cross-section dimension and a pronounced offset increase for type B that is rather indicated in a varus situation. The type G implant was designed to fit the valgus femoral neck shape (Figs. 1 and 2). The goal for this implant system was to restore the physiological biomechanics of the hip joint by remaining the offset and the leg length. This might be a benefit to other designs that do not consider the problems of a varus hip, thus producing an elongated leg length by compensating the loss of offset and consecutive reduced soft tissue tension with a longer neck (Iagulli et al., 2006; Jerosch, 2011; Shiramizu et al., 2004). Another aim of the design was to achieve a better adaption to varus or valgus conditions reducing the 'stress shielding' effect. Finite element (FE) simulations are a widely accepted way to evaluate the proposed stem to address the clinical concerns (Lerch et al., 2012a).

Our study group previously developed a finite element model (FEM) that was validated by a prospective dual energy X-ray absorptiometry (DEXA) trial (Lerch et al., 2012a; Lerch et al., 2012b). Currently, the FEM used in the present study is the most exact model available consisting of only biomechanical data. The great advantage of this computational method is that it can provide bone remodeling data and stress patterns before an implant is inserted (Behrens et al., 2009; Kerner et al., 1999; Kuiper and Huiskes, 1997). Our numerical model can be used to aid in the development of novel implants or to detect possible hazards of a new implant in a 'pre-launch' investigation. As patient safety is of increasing interest and an increasing number of new implants with various designs are being developed (Falez et al., 2015),

there is a need for a reliable tool to investigate the eligibility of new implants before they are inserted in patients. We furthermore have the possibility to simulate clinical relevant problems such as inappropriate implant selection or under/oversizing. These conditions result in an incongruous implant and might lead to femoral bone loss due to non-physiologic load transfer and associated stress-shielding (Goetzen et al., 2005; Gotze et al., 2010; Lerch et al., 2013a). However, there is no data available of the effect of an incongruous implant on bone remodeling.

We asked the following research questions: (i) Can we detect possible adverse effects on bone remodeling? (ii) Is the overall bone density reduction acceptable? (iii) What effect would an incongruous implant have on bone remodeling patterns (imperfection scenario)?

2. Methods

We investigated a novel A2 short-stemmed THA femoral implant. This implant has a metaphyseal, intertrochanteric fixation and load transfer. Indications are primary and secondary osteoarthritis, medial fracture of the femoral neck, and avascular necrosis of the femoral head. There is no age limitation. Contraindications for the A2 stem are acute or chronic local or systemic infection, severe diseases of the muscles, bones and/or nervous system, severe bone density impairment, large bone defects (revision arthroplasty), and pronounced coxa valga or vara (head/neck angle $> 145^{\circ}$ or $< 120^{\circ}$). The indication is critical in obese patients (BMI > 30) and in cases with developmental dysplasia of the hip, pronounced antetorsion, and/or a wide femoral neck.

2.1. The implant design rationale

This new implant was developed in an attempt to improve the anatomic fit to the proximal femur by increasing the contact zone with the medial calcar rounding and by implementing offset and leg length reconstruction in the size evolution considering the varus or valgus hip. This was realized by assessing offset and leg-length problems with the use of the Metha short hip stem (BBraun, Aesculap, Tuttlingen, Germany) and the Nanos stem (Smith & Nephew Orthopedics, Tuttlingen, Germany). After numerous X-ray templatings with these implants, the developers of the A2 system realized that only an implant with two bodies could resolve these issues; this is called the two-body philosophy. The A2 implant system consists of two base bodies (types B and G), which differ in the neck angle, medial calcar contact area, and angle of the tip of the prosthesis (Fig. 1). Furthermore, the implant has a threefold conical shape, a cylindrical cross section, is made of proximal coated titanium (Ti6Al4V) forged alloy (ISO 5832-3), and has an additional calcium phosphate layer in the proximal rough aspect of the stem (Fig. 2). Every implant body has a colour code (type B is blue and type G is yellow), which is consistent from templating to the instrument to final implant insertion. There are currently 10 sizes available per body (0–9).

2.2. The finite element model

The finite element analysis (FEA) method and the validation study have been already described (Behrens et al., 2017; Lerch et al., 2012a; Lerch et al., 2012b): A Surface Triangulation Language model based on CT data of a 75 kg male patient was generated by means of 3D medical image processing and editing software (Mimics, Materialize, Leuven, Belgium). A solid FE model was built based on 10-noded tetrahedral elements using the preprocessor HyperMesh (Altair Engineering GmbH, Böblingen, Germany) (Behrens et al., 2009). The apparent bone density (ABD) distribution from the measured Hounsfield Unit (HU) values was calculated according to Rho et al. (Rho et al., 1995). We conducted a three-dimensional preoperative planning procedure and positioned the implant as per the manufacturers' instructions. The implant body G showed the best fit, and was thus chosen for the stem-femur composite (Fig. 3a).

The prosthesis is made of titanium forged alloy (Ti6Al4V/ISO 5832-3); thus, it was modelled as homogenous and isotropic with an elastic modulus of $E = 110$ GPa and Poisson's ratio of $\upsilon = 0.3$. The stem has a proximal rough titanium, micro-porous coating. This was modelled that no relative stem-bone motion was possible. Although minimal physiological micromotion will probably occur, even in the proximal coated area, until secondary osseointegration has finished (Karrholm et al., 1994), we simulated full bonding with a friction coefficient of 1 between the bone and the coated area, as this most closely approximates the state of osseointegration of the surface (Biemond et al., 2011). Physiological loading conditions were simulated using the boundary conditions described by Speirs et al. (Speirs et al., 2007a) and by simulating the entire gait cycle (the most frequent activity of a THA patient (Morlock et al., 2001) of the hip (Bergmann et al., 2001). Contact forces and muscle forces were taken from previous clinical investigations (Bergmann et al., 2001), (Duda et al., 1997). As shown in former studies (Bitsakos et al., 2005; Duda et al., 1998) that showed the influence of muscle forces on load distribution, a reduced muscle system (Heller et al., 2005) was used, consisting of the abductor muscles, the M. tensor fascia latae, the M. vastus medialis and the M. vastus lateralis.

We applied a bone adaption law that was inaugurated in 1892 (Wolff, 1986) and was modified by our study group to build in a saturation function with an integrated osteonecrosis effect when bone loads exceeded defined limits (Behrens et al., 2009; Lerch et al., 2012a):

The physiological loading pattern in the intact femur under the considered loading history was calculated in one cycle and the changes in material properties (ABD and modulus) of the bone in the femur after THA were determined. This iterative process ends when the change in the bone mass converges. Bone remodeling was calculated by quantifying the change in the ABD using the adaptation law. It was implemented in the FE solver MSC.MARC (MSC.Software Corporation, Santa Ana, CA). The value for the dead zone z, where changes in load distribution do not cause remodeling, was defined as $z = 75\%$. The threshold level for severe overloading ($\xi > y$) causing bone necrosis was $y = 400\%$.

The overall bone mass loss as well as the ABD distribution in the modified Gruen zones was computed (Falez et al., 2008; Speirs et al., 2007b) (Fig. 3a).

2.3. The DEXA validation study

The prospective clinical DEXA validation study was previously described (Lerch et al., 2012a; Lerch et al., 2012b): In brief, a series of 25 patients with unilateral Metha® stem (BBraun, Aesculap, Tuttlingen, Germany) implanted by three experienced senior surgeons over a standard lateral approach in the supine position were included. Mean age was 58.9 years (range 38–69 years) and mean preoperative BMI was 24.6 (range 20.6–27.4).

Bone mineral density (BMD, g/cm^2) data collected one week after surgery served as baseline value for the following DEXA examinations. All patients had full weight bearing postoperatively. DEXA scans were performed using a HOLOGIC Discovery A S/N 80600 device (Hologic Inc., Waltham, MA). The BMD of the operated hip was measured using the “metal-removal” scanning mode. Conventional Gruen's zones were adapted to the short stem design (Falez et al., 2008; Roth et al., 2005; Speirs et al., 2007b).

For displaying the results of the validation we took the data from our previous FEA and DEXA studies (Lerch et al., 2012a; Lerch et al., 2012b), calculated the changes of the FEA in the 7 Gruen Zones and compared them to the changes in the DEXA. The FE calculations showed bone mass loss in the proximal regions. In the distal femur, no change in distribution of ABD was calculated. This observation corresponded to the DEXA results. In accordance with the FEA, we found a BMD decrease in the greater trochanter (Lerch et al., 2012a). The DEXA

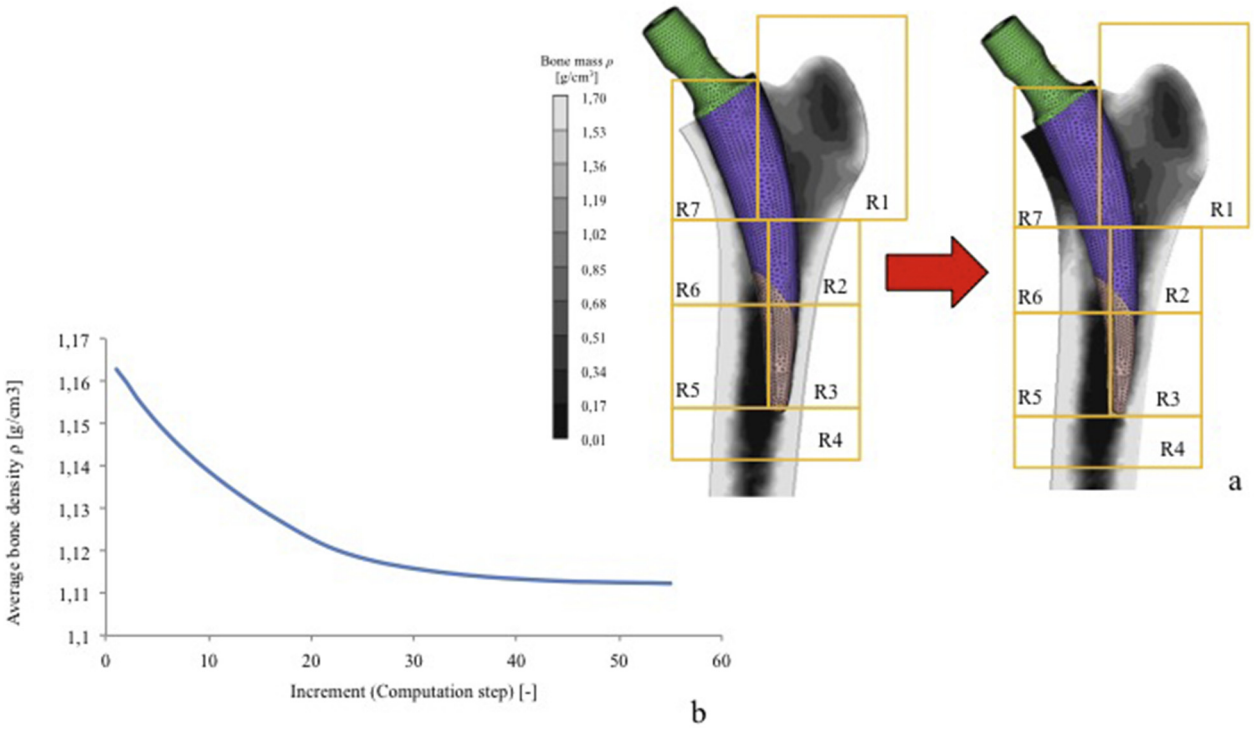

Fig. 3. The qualitative results of the simulation with the apparent bone density distribution in the periprosthetic femur directly after implantation (on the left) and after reaching the final state (on the right) (a). Note the modified Gruen zones for the quantitative analysis. The initial state at increment 1 represents the direct postoperative situation, and increment 53 represents the final state when equilibrium was reached (b).

investigation showed a strong increase in bone mineral density in the medial calcar region (Gruen zone 7). As we described in our previous validation study, we found a scan area reduction of 36% in Gruen zone 7 and implemented this in the calculation of the validation results (Lerch et al., 2012a). Thus, the FE results in the 7 Gruen zones deviated by 10,0% (range 5,3%–20,0%) from the DEXA results.

2.4. The imperfection scenario

We computed an imperfection scenario by implanting a type B implant that would not be appropriate clinically for the femur model that was used (Fig. 4a). The type B implant was oversized in the proximal calcar ring so that cortical bone would need to be resected and consequently weakened. Furthermore, the fitting to the medial calcar region was not as good with the type B implant as with the type G implant, making the type B implant too bulky in the subtrochanteric area.

3. Results

Equilibrium was reached after 53 computation steps, when the bone density did not decrease > 0,005 g/cm^3 per simulation step (Fig. 3b). Overall bone mass loss was 4.3% for the entire femur. The ABD

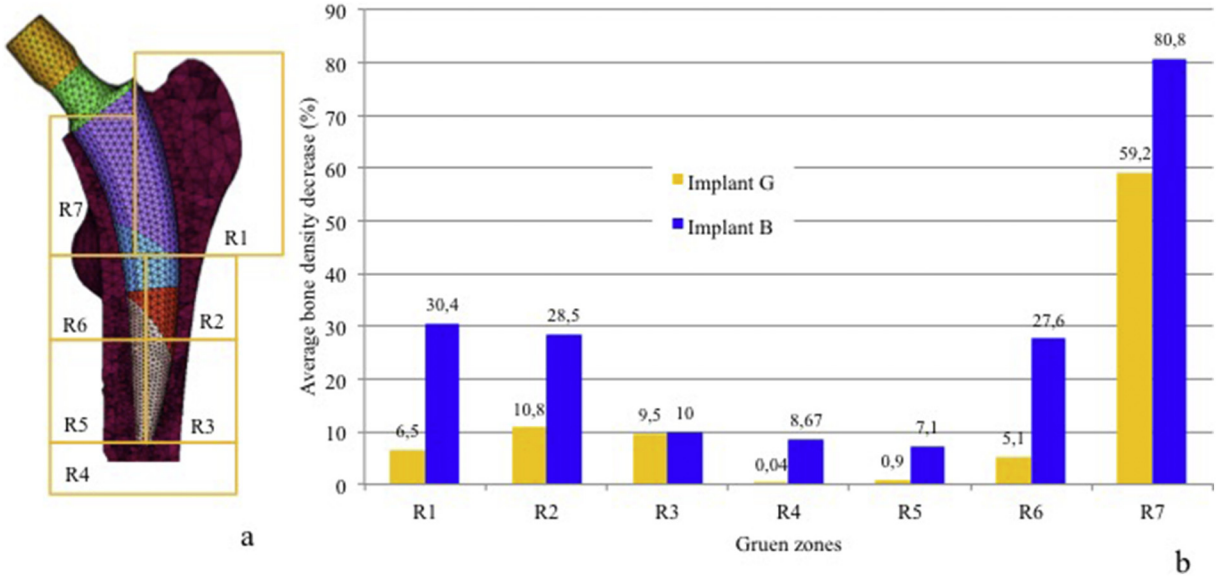

Fig. 4. The imperfection scenario (a) with the implant body B shows the oversizing in the proximal calcar ring. (b) Direct comparison of the average bone density decrease of the two implants in the femur model shows a pronounced increase in bone mass reduction in all zones except for Gruen zone 3 for implant type B.

Table 1
Bone mass reduction in the Gruen zones during simulation of type G implant.

Gruen zone	1	2	3	4	5	6	7
Bone mass reduction [%]	6,5	10,8	9,4	0,04	0,8	5,1	59

distribution in the Gruen zones is displayed in Fig. 3 and Table 1. There was a pronounced increase in ABD in the lateral aspect of the cortical ring. Signs of stress shielding were observed in the calcar region. There was no change in ABD in the diaphysis and around the tip of the implant.

3.1. The imperfection scenario

Direct comparison of the two implants in the femur model showed that implant type B resulted in a stronger increase in bone mass reduction in all zones except for Gruen zone 3 (Fig. 4b).

4. Discussion

The present FEA did not show any deviations or inexplicable phenomena. The overall bone mass loss and the ABD patterns are comparable to those of our previous short-stem implant investigations (Lerch et al., 2012a; Lerch et al., 2013a). The ABD reduction in the proximal calcar region was only little greater compared with the previous investigations of the Metha and Nanos stems (Lerch et al., 2012a; Lerch et al., 2013a); this is noteworthy, as the coated zone of the A2 implant reaches significantly further distally than the abovementioned stems, especially in the lateral aspect of the stem, potentially causing more stress shielding. In the development of the A2 implant, this increased coated zone was accepted to increase the rotational stability; another possible explanation could be the sensitive computation method. The difference in simulated bone mass change was so slight that it might also have resulted from the particular way that the implant was implanted in the femur model. The imperfection scenario (Fig. 4) supports this assumption. However, the bone mass increase in the lateral cortical region was more accentuated compared with all other implants investigated. We know from previous examinations that this is an important sign for correct load distribution of the short-stemmed implant; the support at the lateral cortical ring prevents the implant from valgus migration and promotes a more physiological loading pattern. Another indication of stress shielding reduction is the absence of distal bone mass increase. In contrast to the Nanos stem, a wedge fixation in the metaphysis cannot be noted. Arabnejad et al. recently published the computational results after implantation of a short-stem taper-wedge implant made from high strength fully porous material with tunable mechanical properties (Arabnejad et al., 2016); they compared a three-dimensional printed fully porous hip implant with a conventional implant made of solid material. Interestingly, using a porous stem with tuned mechanical properties reportedly reduced the stress shielding by 75% in the calcar (Arabnejad et al., 2016). This might indicate that besides the ideal load distribution of the implant, the stiffness of the material could be more important than previously thought. To our concerns this should be regarded when comparing solid implants with different diameters or implant body geometries as this also affects elasticity.

The imperfection scenario in our study showed enormous differences in ABD that cannot be justified by increased bone resection during virtual implantation; this might indicate the sensitivity of the model system in response to modifications of implant positioning. This can be supported by the findings of Burchard et al. who showed that the level of osteotomy and therefore bone resection did not affect stress shielding in short stem THA (Burchard et al., 2017). The ABD in the imperfection scenario is similar to that of a straight stem we investigated in a previous study (Lerch et al., 2012b; Lerch et al., 2013a), indicating a rather distal fixation. In some clinical cases this could be a desired effect, but this is not the first line intention of the A2 implant system. Due to the large implant size in the imperfection scenario, the pronounced proximal bone mass decrease could be a sign of stress shielding due to rigid buttressing in this area. Furthermore, the imperfection scenario might indicate that both undersizing *and* oversizing of the implant can lead to unsatisfactory results, and therefore proper implant selection is crucial in clinical practice. However, the more severe problem is periprosthetic fracture during implantation of an oversized implant, which cannot be simulated with our model. However, based on the computational data further statements concerning the issue of periprosthetic fracture during stem insertion would be speculative. It has to be noted that the present results can probably not be transferred to any other implant with different loading patterns. At this point a variation of strain and stress types and implant modification to compare the impact of different geometry designs could be interesting. However, implant development or improvement was not the intention of the present study.

Although we have extensive clinical experience of over 15 years with short-stemmed implants such as the Metha stem and the Nanos stem, we had not previously used the A2 implant system, as the present study was conducted before the implant was introduced. As a consequence, we cannot compare the numerical results with clinical experience. In future we need to collect clinical data to compare with the numerical data presented in this paper. However, the major reason for the present study was the promising design of the implant, which is appealing to us as we are already Metha stem users. We are aware of the few problems with the Metha and Nanos stems (offset, stem position, size evolution, and calcar fit). During our learning curve, we were able to solve these problems mainly by critical patient selection for the discussed implants. The A2 implant system addressed these problems, and so the A2 implant might be regarded as a logical and consequent development of the established short-stem designs. However, we need clinical experience to finally assess the A2 implant. The next logical step in implant development would be backward computation from our numerical model. This brings back the idea of patient-specific implant development, which should not be discussed here. However, the two-body design of the A2 implant gives good modularity in a monoblock system that can address a range of femoral variations.

Some limitations of the study have to be noted. As the application of the method to short stemmed implants and the implant itself are relatively new, we are not able to define „hard “targets or aims on how the implant has to affect the bone. We can only approximate by looking at other comparable implants. An adverse effect would be a substantial deviation from loading, remodeling patterns and “accepted” bone density reductions we know from other investigations on short stems. We cannot define “the ideal” remodeling as we always need to deal with bone density reduction with every implant.

The numerical methodology is based on pure mechanical analysis of the bone tissue under the load of the hip contact forces after implanting the prosthesis. This mechanical analysis does not take into account the biological, biochemical and individual conditions in the human body. These factors may indeed represent important limitations of the numerical model, as they may also affect bone remodeling. Since the prosthesis' design affects mostly the biomechanical aspects (Mulier et al., 2011; Pitto et al., 2010), we can establish conclusions using our FE-Model. The direct quantitative comparison between the simulation and the DEXA results has to be regarded very carefully. Although studies showed that bone remodeling plateaus after 2 years after implantation of straight stems (Aldinger et al., 2003; Boden et al., 2006; Brodner et al., 2004), we cannot act on the assumption that this will be the case in short stem THA (Lerch et al., 2012a).

In our study we assumed a very high friction coefficient to avoid inaccuracy in contact conditions since our intention was to study the influence of the prosthesis's design. In a previous study we investigated the influence of the size of the implant and different coating principles

(Behrens et al., 2017). We thus modified the contact conditions and the implant was modelled with a contact friction coefficient of $\mu = 0.65$ with the bone tissue, whereas the uncoated area of the implant has a friction coefficient value of $\mu = 0.01$.

We modelled only one physiological femur geometry; hence, we cannot predict how different femur morphologies would remodel under the influence of the A2 implant. The most important and time- and money-consuming procedure in FE is the development of a representative model. This took most of the available capacity for the study's subproject. However, a next step must be the development of typical pathological femur models to aid the surgeon in defining the limits of an implant. Also, relevant patient-related factors (obesity; osteoporotic bone stock) were not included in the model; however, they might be important when defining the comparability and maybe the longevity of the implant. The data available for computing these biological factors is vague and would have caused some bias and weakened the model's predictability. These limitations where already discussed in detail in previous publications dealing with this femur model (Lerch et al., 2012a; Lerch et al., 2013a; Lerch et al., 2013b). Furthermore, our model assumes a complete osseous integration of the stem. Therefore, this testing method cannot detect early aseptic loosening, due to inadequate osseous integration. It was not our intention to model initial periprosthetic tissue healing or problems with the bone-implant interface. This would be an interesting approach, but in the present story we focus on normal or “ideal” course of healing in a standard patient. We rather see mechanical factors leading to changes in bone remodeling then problems with periprosthetic tissue healing which may occur during the early postoperative time. These patients may have a loose implant, which results in early bone loss, pain and loss of function even before we see stress shielding. This can be one of the primary failure mechanisms of all short stem implants and must be taken into account to assess clinical safety prior to component introduction. The strength of the present study is that it is validated against an in vivo DEXA study (Lerch et al., 2012a; Lerch et al., 2012b), seen as the “gold standard” (Brodner et al., 2004; Lerch et al., 2013b) as recommended by Viceconti et al. (Viceconti et al., 2005).

Although this theoretical study produced promising results, we strongly recommend waiting for reliable clinical data before expanding the indications for the investigated implant system. We would like to emphasise that no theoretical approach to rate implant function and impact should replace a clinical observational study.

5. Conclusions

This finite element study could not detect any adverse effects of the A2 short-stemmed implant system on bone remodeling. The overall bone density reduction was acceptable, considering that the A2 implant has a relatively extended coated area. Wedge fixation was not observed, indicating no distal load transfer. The simulation of an incongruous implant indicates the sensitivity of our model in response to modifications of implant positioning. Furthermore, it shows that undersizing of the implant can lead to unsatisfactory results, and that oversizing should also be avoided using the A2 system.

Funding

This research was supported by ImplanTec Germany, Lüdinghausen, Germany.

Conflicts of interest

One author (Matthias Lerch) has received a speaker honorarium from ImplanTec. The Institute of Forming Technology and Machines at the Leibniz University Hannover received research grants from ImplanTec. Author Henning Windhagen, Author Agnes Kurtz, and Author Stefan Budde declare that they have no conflict of interest.

Ethical approval

This article does not contain any studies with human participants or animals performed by any of the authors.

CRediT authorship contribution statement

Matthias Lerch: Conceptualization, Investigation, Funding acquisition, Writing - original draft, Writing - review & editing. **Henning Windhagen:** Writing - original draft, Writing - review & editing. **Agnes-Elisabeth Kurtz:** Writing - original draft, Writing - review & editing. **Stefan Budde:** Writing - original draft, Writing - review & editing. **Bernd-Arno Behrens:** Formal analysis, Conceptualization, Investigation, Writing - original draft, Writing - review & editing. **Anas Bouguecha:** Formal analysis, Conceptualization, Investigation. **Amer Almohallami:** Conceptualization, Writing - original draft, Writing - review & editing, Investigation, Software.

References

Aldinger, P.R., Sabo, D., Pritsch, M., Thomsen, M., Mau, H., Ewerbeck, V., Breusch, S.J., 2003. Pattern of periprosthetic bone remodeling around stable uncemented tapered hip stems: a prospective 84-month follow-up study and a median 156-month cross-sectional study with DXA. Calcif.Tissue Int. 73, 115–121.

Arabnejad, S., Johnston, B., Tanzer, M., Pasini, D., 2016. Fully porous 3D printed titanium femoral stem to reduce stress-shielding following total hip arthroplasty. J. Orthop. Res. 35, 1774–1783.

Behrens, B.A., Nolte, I., Wefstaedt, P., Stukenborg-Colsman, C., Bouguecha, A., 2009. Numerical investigations on the strain-adaptive bone remodelling in the periprosthetic femur: influence of the boundary conditions. Biomed. Eng. Online 8, 7.

Behrens, B.A., Bouguecha, A., Lerch, M., Windhagen, H., Almohallami, A., 2017. Influence of hip prosthesis size and its coating area on bone remodeling. IEEE Trans. Nanobioscience 16, 703–707.

Bergmann, G., Deuretzbacher, G., Heller, M., Graichen, F., Rohlmann, A., Strauss, J., Duda, G.N., 2001. Hip contact forces and gait patterns from routine activities. J. Biomech. 34, 859–871.

Biemond, J.E., Aquarius, R., Verdonschot, N., Buma, P., 2011. Frictional and bone ingrowth properties of engineered surface topographies produced by electron beam technology. Arch. Orthop. Trauma Surg. 131, 711–718.

Bitsakos, C., Kerner, J., Fisher, I., Amis, A.A., 2005. The effect of muscle loading on the simulation of bone remodelling in the proximal femur. J. Biomech. 38, 133–139.

Boden, H.S., Skoldenberg, O.G., Salemyr, M.O., Lundberg, H.J., Adolphson, P.Y., 2006. Continuous bone loss around a tapered uncemented femoral stem: a long-term evaluation with DEXA. Acta Orthop. 77, 877–885.

Brodner, W., Bitzan, P., Lomoschitz, F., Krepler, P., Jankovsky, R., Lehr, S., Kainberger, F., Gottsauner-Wolf, F., 2004. Changes in bone mineral density in the proximal femur after cementless total hip arthroplasty. A five-year longitudinal study. J. Bone Joint Surg. Br. 86, 20–26.

Burchard, R., Braas, S., Soost, C., Graw, J.A., Schmitt, J., 2017. Bone preserving level of osteotomy in short-stem total hip arthroplasty does not influence stress shielding dimensions - a comparing finite elements analysis. BMC Musculoskelet. Disord. 18, 343.

Duda, G.N., Schneider, E., Chao, E.Y., 1997. Internal forces and moments in the femur during walking. J. Biomech. 30, 933–941.

Duda, G.N., Heller, M., Albinger, J., Schulz, O., Schneider, E., Claes, L., 1998. Influence of muscle forces on femoral strain distribution. J. Biomech. 31, 841–846.

Falez, F., Casella, F., Panegrossi, G., Favetti, F., Barresi, C., 2008. Perspectives on metaphyseal conservative stems. Ital. J. Orthop. Traumatol. 9, 49–54.

Falez, F., Casella, F., Papalia, M., 2015. Current concepts, classification, and results in short stem hip arthroplasty. Orthopedics 38, S6–13.

Goetzen, N., Lampe, F., Nassut, R., Morlock, M.M., 2005. Load-shift–numerical evaluation of a new design philosophy for uncemented hip prostheses. J. Biomech. 38, 595–604.

Gotze, C., Ehrenbrink, J., Ehrenbrink, H., 2010. Is there a bone-preserving bone remodelling in short-stem prosthesis? DEXA analysis with the Nanos total hip arthroplasty. Z. Orthop. Unfall. 148, 398–405.

Heller, M.O., Bergmann, G., Kassi, J.P., Claes, L., Haas, N.P., Duda, G.N., 2005. Determination of muscle loading at the hip joint for use in pre-clinical testing. J. Biomech. 38, 1155–1163.

Iagulli, N.D., Mallory, T.H., Berend, K.R., Lombardi Jr., A.V., Russell, J.H., Adams, J.B., Groseth, K.L., 2006. A simple and accurate method for determining leg length in primary total hip arthroplasty. Am. J. Orthod. 35, 455–457.

Jerosch, J., 2011. Is shorter really better?: philosophy of short stem prosthesis designs. Orthopade 40, 1075–1083.

Karrholm, J., Borssen, B., Lowenhielm, G., Snorrason, F., 1994. Does early micromotion of femoral stem prostheses matter? 4–7-year stereoradiographic follow-up of 84 cemented prostheses. J. Bone Joint Surg. Br. 76, 912–917.

Kerner, J., Huiskes, R., Van Lenthe, G.H., Weinans, H., Van Rietbergen, B., Engh, C.A., Amis, A.A., 1999. Correlation between pre-operative periprosthetic bone density and

post-operative bone loss in THA can be explained by strain-adaptive remodelling. J. Biomech. 32, 695–703.
Kuiper, J.H., Huiskes, R., 1997. The predictive value of stress shielding for quantification of adaptive bone resorption around hip replacements. J. Biomech. Eng. 119, 228–231.
Lerch, M., Kurtz, A., Stukenborg-Colsman, C., Nolte, I., Weigel, N., Bouguecha, A., Behrens, B.A., 2012a. Bone remodeling after total hip arthroplasty with a short stemmed metaphyseal loading implant: finite element analysis validated by a prospective DEXA investigation. J. Orthop. Res. 30, 1822–1829.
Lerch, M., von der Haar-Tran, A., Windhagen, H., Behrens, B.A., Wefstaedt, P., Stukenborg-Colsman, C.M., 2012b. Bone remodelling around the Metha short stem in total hip arthroplasty: a prospective dual-energy X-ray absorptiometry study. J. Orthop. Res. 36, 533–538.
Lerch, M., Weigel, N., Windhagen, H., Ettinger, M., Thorey, F., Kurtz, A., Stukenborg-Colsman, C., Bouguecha, A., 2013a. Finite element model of a novel short stemmed total hip arthroplasty implant developed from cross sectional CT scans. Technol. Health Care 21, 493–500.
Lerch, M., Windhagen, H., Stukenborg-Colsman, C.M., Kurtz, A., Behrens, B.A., Almohallami, A., Bouguecha, A., 2013b. Numeric simulation of bone remodelling patterns after implantation of a cementless straight stem. Int. Orthod. 37, 2351–2356.
Morlock, M., Schneider, E., Bluhm, A., Vollmer, M., Bergmann, G., Muller, V., Honl, M., 2001. Duration and frequency of every day activities in total hip patients. J. Biomech. 34, 873–881.
Mulier, M., Jaecques, S.V., Raaijmaakers, M., Nijs, J., Van der, P.G., Jonkers, I., 2011. Early periprosthetic bone remodelling around cemented and uncemented custom-made femoral components and their uncemented acetabular cups. Arch. Orthop. Trauma Surg. 131, 941–948.
Pitto, R.P., Hayward, A., Walker, C., Shim, V.B., 2010. Femoral bone density changes after total hip arthroplasty with uncemented taper-design stem: a five year follow-up study. Int. Orthod. 34, 783–787.
Rho, J.Y., Hobatho, M.C., Ashman, R.B., 1995. Relations of mechanical properties to density and CT numbers in human bone. Med. Eng. Phys. 17, 347–355.
Roth, A., Richartz, G., Sander, K., Sachse, A., Fuhrmann, R., Wagner, A., Venbrocks, R.A., 2005. Periprosthetic bone loss after total hip endoprosthesis. Dependence on the type of prosthesis and preoperative bone configuration. Orthopade 34, 334–344.
Sano, K., Ito, K., Yamamoto, K., 2008. Changes of bone mineral density after cementless total hip arthroplasty with two different stems. Int. Orthod. 32, 167–172.
Shiramizu, K., Naito, M., Shitama, T., Nakamura, Y., Shitama, H., 2004. L-shaped caliper for limb length measurement during total hip arthroplasty. J. Bone Joint Surg. Br. 86, 966–969.
Speirs, A.D., Heller, M.O., Duda, G.N., Taylor, W.R., 2007a. Physiologically based boundary conditions in finite element modelling. J. Biomech. 40, 2318–2323.
Speirs, A.D., Heller, M.O., Taylor, W.R., Duda, G.N., Perka, C., 2007b. Influence of changes in stem positioning on femoral loading after THR using a short-stemmed hip implant. Clin. Biomech. 22, 431–439.
Stukenborg-Colsman, C.M., von, d.H.-T., Windhagen, H., Bouguecha, A., Wefstaedt, P., Lerch, M., 2012. Bone remodelling around a cementless straight THA stem: a prospective dual-energy X-ray absorptiometry study 2. Hip Int. 22, 166–171.
Tai, C.L., Shih, C.H., Chen, W.P., Lee, S.S., Liu, Y.L., Hsieh, P.H., Chen, W.J., 2003. Finite element analysis of the cervico-trochanteric stemless femoral prosthesis. Clin. Biomech. 18, S53–S58.
Taylor, W.R., Ploeg, H., Hertig, D., Warner, M.D., Clift, S.E., 2004. Bone remodelling of a proximal femur with the thrust plate prosthesis: an in vitro case. Comput. Methods Biomech. Biomed. Engin. 7, 131–137.
Viceconti, M., Olsen, S., Nolte, L.P., Burton, K., 2005. Extracting clinically relevant data from finite element simulations. Clin. Biomech. 20, 451–454.
Wolff, J., 1986. 1892. Das Gesetz der Transformation der Knochen. Springer.